Dynamics of protonic conductors $Rb_3H(SO_4)_2$ and $Rb_3D(SO_4)_2$ studied by NMR

J. Dolinšek, U. Mikac, J. E. Javoršek, G. Lahajnar, and R. Blinc
J. Stefan Institute, University of Ljubljana, Jamova 39, SLO-1000 Ljubljana, Slovenia

L. F. Kirpichnikova
Shubnikov Institute of Crystallography, Russian Academy of Sciences, Leninskii pr. 59, Moscow, 117333 Russia
(Received 18 March 1998; revised manuscript received 25 June 1998)

The dynamics of $Rb_3H(SO_4)_2$ and $Rb_3D(SO_4)_2$ crystals has been studied between 4 K and the superionic phase ($T_c \approx 448$ K). ^{87}Rb and deuteron NMR spectra exhibit motional narrowing on heating whereas the spin-lattice relaxation (T_1) rates behave in an unusual way—they increase on cooling in the whole investigated temperature range but show no frequency dependence. Such a behavior can be explained by the phonon-induced relaxation via Raman processes. The results demonstrate that the dynamics of the above systems is predominantly determined by the thermally induced SO_4 vibrations, torsional oscillations, and reorientations resulting from the high elasticity of the crystal structure. Lattice vibrations dominate crystal dynamics in a large temperature range from the superionic phase down to as low as 20 K. In addition the deuteron soft-mode slowing-down dynamics has been observed close to the antiferroelectric transition in the deuterated compound. The deuteron two-dimensional exchange NMR experiment has detected the deuteron interbond motion as a precursor of the superionic conductivity already at room temperature which is as much as 170 K below the superionic phase transition. [S0163-1829(98)04838-3]

I. INTRODUCTION

The $M_3H(XO_4)_2$ family of hydrogen-bonded insulators, where $M=$ K, Cs, Rb, NH_4 and $X=$ S, Se, has attracted a lot of attention due to an unusually large isotope effect on deuteration found in the antiferroelectric transition temperature and the occurrence of the superionic conductivity at high temperatures. The fundamental question is why the three protonated crystals[1] $K_3H(SO_4)_2$, $Rb_3H(SO_4)_2$, and $Rb_3H(SeO_4)_2$ do not exhibit any phase transition down to the lowest measured temperatures in spite of their apparent isostructure with the deuterated analogs which undergo an antiferroelectric transition [e.g., at 84 K in $K_3D(SO_4)_2$ and 82 K in $Rb_3D(SO_4)_2$]. The study of the partially deuterated crystals $K_3D_{1-x}H_x(SO_4)_2$ (Refs. 2, 3), $Rb_3D_{1-x}H_x(SO_4)_2$ (Ref. 4), and $Rb_3D_{1-x}H_x(SeO_4)_2$ (Ref. 4) has shown that the critical temperature T_c of the antiferroelectric transition decreases with increasing proton concentration and the phase transition vanishes when the concentration x exceeds the critical value x_c. Dielectric and specific heat measurements[3,4] yielded the critical concentrations $x_c = 0.66$, 0.78, and 0.96, respectively, for the above three compounds.

The origin of the anomalous isotope effect has been discussed in different ways. It is apparent that the isotope effect is strongly related to the specific crystal structure which contains a ''zero-dimensional'' hydrogen-bond network[5] consisting of isolated SO_4^{2-}-H$\cdots$$SO_4^{2-}$ dimers, which can be to a good approximation treated as noninteracting. One possible explanation has been given in terms of the geometrical isotope effect.[6,7] The protonated hydrogen bond is somewhat shorter than the deuterated one. These crystals exhibit a significant thermal contraction on cooling[8,9] and the monotonic decrease of the lattice parameters induces a monotonic decrease of the H-bond length.[10] It was suggested[7] that the length of the protonated bond accidentally crosses the critical bond length of 2.47 Å at about 100 K, where a double-minimum H-bond potential transforms into a single minimum so that the ordering of protons between two off-center equilibrium sites is no more possible. The crossing of the critical length does not occur in the deuterated compound due to the larger deuteron bond length so that the order-disorder phase transition is there preserved.

The hypothesis of a single-minimum potential is not supported by the Raman scattering study[3] of the partially deuterated $K_3D_{1-x}H_x(SO_4)_2$ system. The study of the ν_2 modes in samples with various degrees of deuteration has shown the existence of three lines $\omega(SO_4^{2-})$, $\omega(HSO_4^-)$, and $\omega(DSO_4^-)$ down to the lowest measured temperatures (15 K), demonstrating the existence of two off-center sites in both the protonated and the deuterated H-bond potentials. Both potentials thus appear to be of a double-minimum type.

Another possible explanation of the vanishing phase transition in protonated compounds has been given by the hypothesis of an intense proton tunneling.[11,2] The tunneling rate strongly depends on the barrier height in the double potential. This height in turn depends on the H-bond length which is shorter in the protonated case. It was considered that the barrier is small enough in the protonated samples so that the intense proton tunneling suppresses the phase transition, whereas this is not the case in the deuterated samples. One is thus dealing with a quantum phase transition which again depends on the geometrical effect. It was pointed out[2] that the dimer structure of the $M_3H(XO_4)_2$ crystals realized by only a single H bond between two SO_4 tetrahedra makes these systems almost ideal to study the proton tunneling motion in solids. The dimension of the H-bond network is here fundamentally different from that in the other investigated H-bonded insulators. In the $PbHPO_4$ family there exist one-

 © 1998 The American Physical Society

dimensional (1D) H-bonded chains, squaric acid contains a 2D planar network and the KDP family a 3D network. In these structures there exist correlations between the motions in the neighboring bonds and the Pauling ''ice rules'' do not allow one proton to tunnel independently of the others. In the $M_3H(XO_4)_2$ family, on the other hand, the H-bond network is ''zero dimensional,'' the ice rules do not apply, and the tunneling in a given bond can be to a good approximation treated as independent from the motion in the other bonds.

The hypothesis of a quantum phase transition suppressed by fast tunneling, which is at least at low temperatures expected to occur only within the ground state doublet of a double minimum potential, is not supported by the inelastic neutron scattering (INS) experiment[12] on $K_3H(SO_4)_2$ and $Rb_3H(SO_4)_2$. Unlike Raman scattering, which probes the SO_4^{2-} and lattice vibrations, INS is sensitive to proton modes and has provided a clear evidence that the H-bond potentials are of an asymmetric double minimum type down to 2 K with the barrier height of 83 MeV in $K_3H(SO_4)_2$ and the ground state doublet ($0\rightarrow1$ transition) splitting of 7.1 meV. The wave functions of the two lowest states were found practically localized in each well so that the tunneling within this doublet is negligible. The transitions between the two lowest states have however been clearly observed by INS and it was suggested that the proton transfer is a thermally activated process down to the lowest measured temperatures, thus contradicting the pure quantum nature of the phase transition suppression. INS results also rule out the possibility of a phonon-assisted tunneling of protons within the ground state doublet at low temperatures. In the phonon-assisted tunneling approach the barrier height, and, therefore, the tunnel splitting are modulated by the hydrogen-bond modes. The INS spectra of $K_3H(SO_4)_2$ and $Rb_3H(SO_4)_2$ have shown that the $0\rightarrow1$ splittings which govern the proton transfer at low temperatures, are not coupled to any phonon (no broadening of the bands was observed) and there is no change in the potential barrier between 100 and 2 K so that the phonon-assisted tunneling concept in the ground state doublet does not apply here. This, however, does not rule out the possibility of a phonon-assisted proton transfer over the excited states. The INS-determined energy levels of a proton in the H-bond double potential show localization only for the ground state doublet whereas all the excited states lie above the barrier. The concept of phonon-assisted tunneling over the excited states (which reduces to classical hopping over the barrier when the excited levels lie far above the barrier) could explain the observed thermally activated proton intrabond motion and the suppression of the phase transition in the investigated systems.

There exists another interesting physical phenomenon in the above compounds to which much less attention has been given so far. This is the occurrence of the superionic conducting phase at high temperatures. The transition to the superionic phase occurs at practically the same temperature $T_c\approx448$ K in $Rb_3H(SeO_4)_2$ (Refs. 13–15), $Rb_3H(SO_4)_2$, and $Rb_3D(SO_4)_2$. A ^{87}Rb NMR study of the superionic phase in $Rb_3H(SeO_4)_2$ has shown[15] that the superionic transition involves a breakup of the SeO_4-H$\cdots$$SeO_4$ dimers and the formation of a dynamic two-dimensional H-bonded network formed by the reorienting $HSeO_4$ groups in the *ab* plane.

In this paper we show that both phenomena—the low-temperature thermally activated proton intrabond transfer and the high-temperature superionic conductivity (protonic interbond transfer)—originate from the same dynamic mechanism of thermally activated vibrations and reorientations of the SO_4 tetrahedra. The ^{87}Rb and ^{2}H NMR spin-lattice relaxation and line-shape measurements in $Rb_3H(SO_4)_2$ and $Rb_3D(SO_4)_2$ have shown that these processes determine the dynamics of the system in a large temperature interval from much below the antiferroelectric transition in the deuterated compound up to the superionic phase.

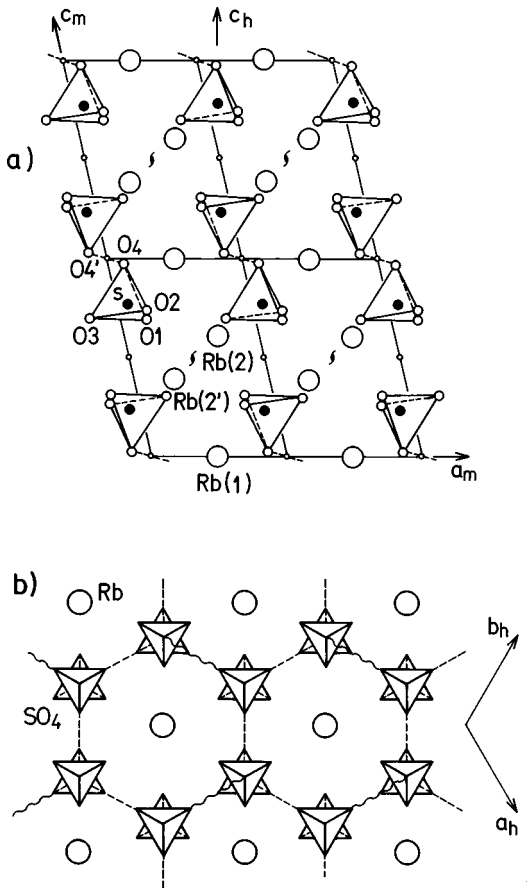

FIG. 1. (a) Room temperature schematic arrangement of atoms in the monoclinic unit cell of $Rb_3H(SO_4)_2$ projected onto the *ac* plane. (b) Schematic arrangement of atoms in the hexagonal structure of the superionic phase projected onto the *ab* plane. The wavy line shows the direction of the given O4-O4′ H bond, while the dashed lines represent the two other possible bonds in the *ab* plane.

II. STRUCTURAL CONSIDERATIONS

$Rb_3H(SO_4)_2$ and $Rb_3D(SO_4)_2$ crystallize at room temperature in the monoclinic space group $A2/a$ [e.g., $a_m=1.0477$ nm, $b_m=0.6086$ nm, $c_m=1.5421$ nm, $\beta=102.92°$, and $Z=4$ for $Rb_3D(SO_4)_2$] and the phase is ferroelastic. The schematic arrangement of atoms in the unit cell projected onto the *ac* plane is shown in Fig. 1(a). One of the three Rb atoms of the formula unit occupies the symmetric Rb(1) site on the twofold axis (parallel to the *b* axis) whereas the other two atoms Rb(2) and Rb(2′) occupy the sites related by a screw axis. A given SO_4-H$\cdots$$SO_4$ dimer consists of two slightly deformed SO_4 tetrahedra. The main frame of the oxygen atoms is almost undistorted, but the sulfur atom

shifts away from the O4 atom so that the SO_4 molecule acquires a spontaneous dielectric polarization P_s. The two SO_4 tetrahedra are connected by a hydrogen bond between the O4 oxygens and the bond lies approximately in the *ab* plane. There are two kinds of dimers with different orientation in the unit cell related by the twofold axis resulting in two differently oriented hydrogen bonds in the *ab* plane. Were the protons located in the middle of the bond, the dimer would possess an inversion symmetry. Since a given SO_4 molecule is connected to another SO_4 by a single H bond only, the tetrahedra possess a high freedom for reorientations in steps of 120° about their local threefold axis passing through the sulfur and the O4 oxygen atom. It was also conjectured that the room temperature phase can be considered as a pseudohexagonal structure due to the fact that the unit cell contains a pseudohexagonal axis [indicated by c_h in Fig. 1(a)] which has the direction of the SO_4 local threefold axis.

In the superionic (paraelastic) phase ($T>448$ K) the atoms slightly displace to more symmetric positions resulting in a symmetrization of the crystal structure. The symmetry is here hexagonal and the space group changes to $R\bar{3}m$. The hexagonal lattice parameters are related to the room-temperature monoclinic ones by $\mathbf{a}_h=\mathbf{a}_m/2-\mathbf{b}_m/2$, $\mathbf{b}_h=\mathbf{b}_m$, and $\mathbf{c}_h=\mathbf{a}_m/2+3\mathbf{c}_m/2$, where $\mathbf{c}_h$ is the threefold axis. The SO_4 tetrahedra are located on this symmetry axis [Fig. 1(b)] and can form three equivalent hydrogen bonds (rotated by 120° in the *ab* plane) to the neighboring SO_4 molecules, out of which only one is populated by a proton. The structure is thus very open. An x-ray study has shown that the O4 oxygens forming the H bonds actually do not lie exactly on the threefold axis but occupy statistically six off-axis positions. This has a consequence that in the reorientation of the SO_4 tetrahedron about this axis a given H-bond length is changing and may be broken so that the proton is transferred to another differently oriented but otherwise equivalent H bond. All three bonds become statistically populated to $\frac{1}{3}$ in the superionic phase. The H-bond system can be thus considered as a dynamic 2D planar network and the ionic conductivity is connected to the motion within this network.

III. EXPERIMENTAL

The dynamics of the proton and deuteron intra- and inter-H-bond transfer has been studied in $Rb_3H(SO_4)_2$ and $Rb_3D(SO_4)_2$ single crystals by ^{87}Rb and ^{2}H NMR. The ^{87}Rb spin-lattice relaxation rates have been measured as a function of temperature by the inversion-recovery method at two Larmor frequencies 124.34 and 88.4 MHz in order to check for the frequency dependence of the relaxation rates. The deuteron spin-lattice relaxation measurements were performed at a frequency 58.3 MHz. The effect of the proton and deuteron interbond motion on the NMR line shape has been studied from low temperatures up to the superionic transition. The ionic mobility results in motional narrowing effects on the quadrupole-perturbed ^{87}Rb and ^{2}H Zeeman spectra. Direct evidence for the slow interbond exchange of deuterons as a precursor of the superionic conductivity has been obtained already far below the superionic transition ($T_c-T\approx 170$ K) by the two-dimensional deuteron exchange NMR technique. Pulsed Fourier transform was used in all measurements. The temperature was stabilized within 0.1 K with an Oxford CF 1200 cryostat.

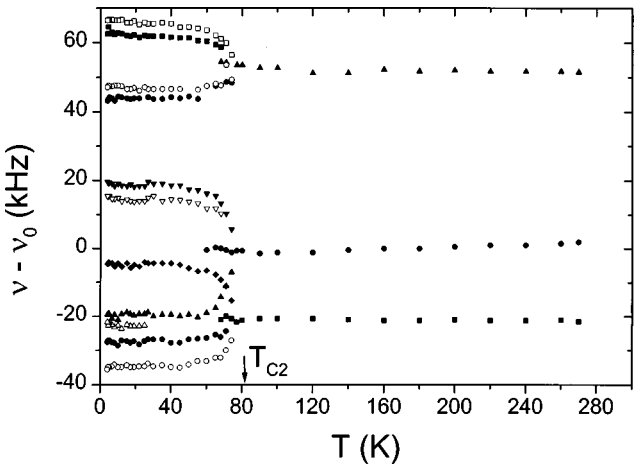

FIG. 2. Temperature dependence of the ^{87}Rb spectral line positions in $Rb_3D(SO_4)_2$ between 280 and 4 K [$\nu_0(^{87}\mathrm{Rb})=124.3$ MHz, orientation $c_m\perp H_0$, $\angle a_m, H_0=15°$].

IV. THE NMR LINE SHAPE

The NMR line shape has been studied in $Rb_3D(SO_4)_2$ as a function of temperature from 4 K up to the superionic transition ($T_{c1}=448$ K). This crystal exhibits at $T_{c2}=82$ K another transition to the antiferroelectric phase. NMR in the deuterated compound has the advantage that the dynamic effects on the line shape can be studied via two resonant nuclei, the ionically bound Rb and the covalently bound deuterons. We analyze the two cases separately.

A. ^{87}Rb spectrum

The ^{87}Rb NMR absorption spectrum (central transition) shows at room temperature three lines. The electric field gradient (EFG) tensors at the Rb(2) and Rb(2′) sites are chemically equivalent due to the screw axis relation of these two sites but nonequivalent with the EFG at the Rb(1) site.

The temperature dependence of the ^{87}Rb spectral line positions in $Rb_3D(SO_4)_2$ between 290 and 4 K is shown in Fig. 2. On cooling from room temperature to the antiferroelectric transition the three lines show a slight monotonic change in frequency following the EFG changes induced by the lattice thermal contraction. At T_{c2} a quadruplication of each Rb line is observed which is consistent with the reported[16] quadruplication of the low-temperature unit cell. The splitting of each line at T_{c2} shows a power-law dependence: $\Delta\nu\propto(T_{c2}-T)^{\beta}$ with $\beta\approx 0.21$. This demonstrates that the changes of the EFG tensor are coupled to the order parameter of the antiferroelectric phase which is here the hydrogen bond polarization p. The above β value is close to that reported by the Raman scattering[3] ($\beta=0.25$).

A remarkable change of the ^{87}Rb spectrum arises when the crystal is heated from room temperature towards the superionic phase (Fig. 3). On heating the individual lines start to broaden continuously and around 400 K a dynamic line-shape transition is observed where the triplet of lines merges into a singlet. This transition occurs at a temperature which is about 50 K lower than the superionic transition tempera-

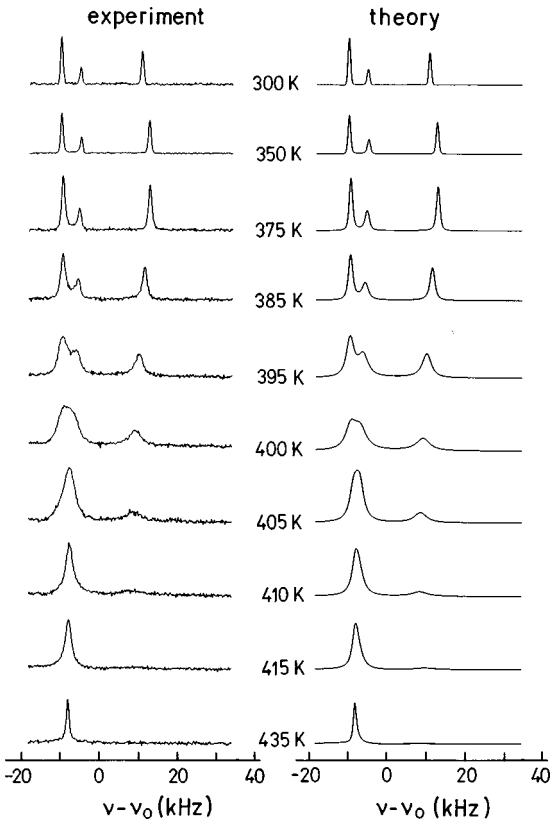

FIG. 3. Temperature dependence of the ^{87}Rb NMR spectrum in $Rb_3D(SO_4)_2$ between room temperature and 435 K (still below the superionic transition). The spectra were measured at $\nu_0(^{87}\mathrm{Rb}) = 124.3$ MHz and orientation $c_m \perp H_0$. The column on the right shows theoretical fits obtained with the three-site exchange model.

ture, i.e., still deeply in the ferroelastic phase. The broadening and merging of the triplet into a single line, which narrows on further heating, represents a typical three-site exchange problem where the absorption frequency of a given resonant nucleus changes between three possible values. Here the three ionically bound Rb nuclei are located at fixed positions in the unit cell but their environment is moving. The EFG tensor at a given Rb site depends predominantly on the orientation of the neighboring SO_4 groups. In the static limit there are three different chemical environments creating three resolved Rb lines. Due to the open crystal structure the SO_4 groups possess a high freedom to perform thermally induced torsional oscillations and reorientations so that at high temperatures all three Rb sites experience the same time-average chemical environment and consequently the same time-average EFG tensor. The triplet of lines thus merges into a singlet located at a time-average resonant frequency. The motional averaging of the local crystal symmetry is a result of the 120° reorientations of the SO_4 tetrahedra about their local pseudothreefold axes. Since the O4 oxygen is not exactly on this axis but slightly displaced, the O4-O4′ distance (determining the H-bond length) dynamically changes during reorientations and the hydrogen bridges get broken. In such a process the protons or deuterons can be exchanged between different SO_4 molecules by a ''hand shaking'' of the rotating tetrahedra, thus inducing ionic charge transport. It is interesting to note that this thermally activated mechanism exists already far below the actual superionic transition. A possible dynamic scenario is that at low temperatures the SO_4 tetrahedra start first to torsionally oscillate. On heating this motion speeds up and increases in amplitude. At still higher temperatures the tetrahedra start to reorient and the reorientational frequencies speed up into the kHz range where they become observable in the frequency window of the NMR line shape experiment. It is straightforward to see that this process does not depend on the deuteration of the H-bonds. This could explain the lack of the isotope effect in the superionic transition temperature [i.e., it is practically the same ($T_c \approx 448$ K) in $Rb_3H(SO_4)_2$, $Rb_3D(SO_4)_2$, and $Rb_3H(SeO_4)_2$].

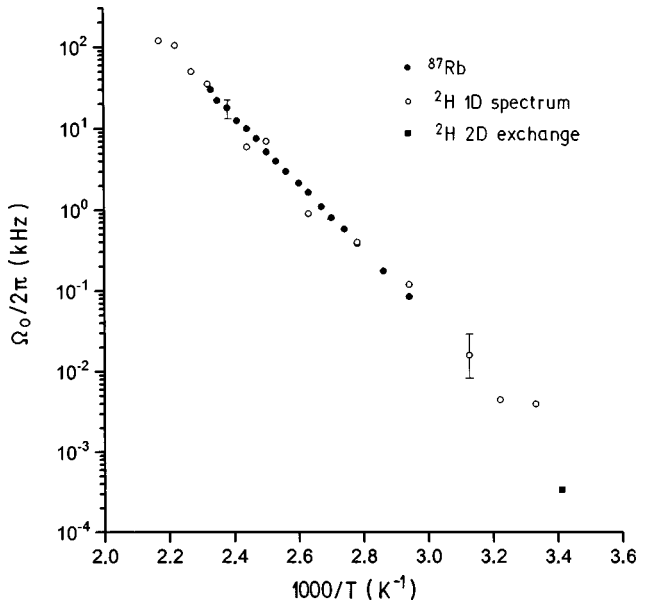

FIG. 4. Temperature dependence of the jump frequency Ω_0 obtained from (a) the ^{87}Rb spectra (solid circles), (b) the deuteron 1D spectra (open circles), and (c) the deuteron 2D exchange experiment (solid square).

The theoretical spectra in Fig. 3 have been obtained by the three-site exchange model of Abragam[17] assuming a jump frequency $\Omega_0 = \tau_{\mathrm{exch}}^{-1}$ for the change of the resonance frequency between the three values. The temperature dependence of Ω_0 is shown in Fig. 4. Ω_0 obeys the Arrhenius thermally activated form $\Omega_0 = \tau_\infty^{-1} \exp\{-E_a/k_B T\}$, with an activation energy $E_a = 0.82$ eV. This high E_a value which demonstrates that heavy objects participate in the dynamics, is consistent with the picture of reorienting SO_4 tetrahedra. At 340 K Ω_0 amounts to $2\pi \times 80$ Hz and speeds up to $2\pi \times 30$ kHz at 435 K just below the superionic phase. Since the SO_4 reorientations are accompanied by deuteron transfer between neighboring H bonds, Ω_0 represents at the same time also the frequency of deuteron interbond exchange.

B. Deuteron spectrum

The EFG tensors of the ionically bound Rb nuclei are determined by the positions of electric charges of many nearby SO_4 tetrahedra so that the Rb nuclei feel the H-bond and SO_4 arrangement inside a relatively large crystal volume. The covalently bound deuterons are, on the other hand, more site specific as their EFG is determined largely by the nearest oxygen atoms, forming a given O-D···O bond, and the sulfur

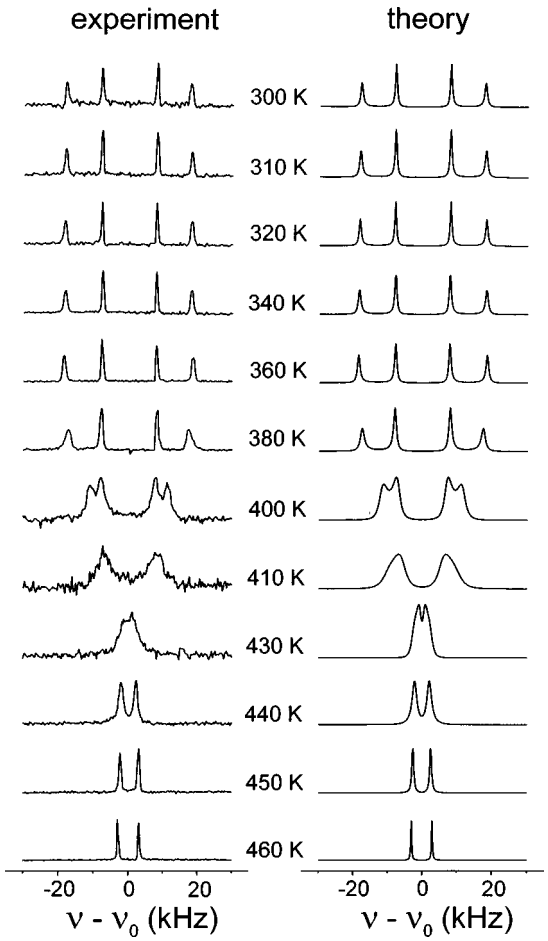

FIG. 5. Temperature dependence of the deuteron NMR spectrum in $Rb_3D(SO_4)_2$ between room temperature and 460 K [$\nu_0(^2H) = 41.463$ MHz, orientation $c_m \perp H_0$, $a_m \| H_0$]. The motional line shape transition takes place already below the superionic phase and no changes are observed on crossing $T_{c1} \approx 448$ K. The column on the right shows theoretical fits obtained with the two-site exchange model.

atoms in the centers of the sulfate tetrahedra. Deuterons thus predominantly see what is happening within the H bond.

The deuteron quadrupole perturbed Zeeman spectra were measured between 300 and 460 K (Fig. 5). At room temperature there are two kinds of deuteron bonds in the unit cell resulting in two pairs of satellite lines. At 300 K the deuteron intra-H-bond motion is fast enough to motionally average the EFG tensors of the two off-center sites in a given bond so that each bond contributes one pair of satellite lines to the spectrum. On heating the two physically nonequivalent lines start to broaden and then merge into a single line resulting in a single pair of satellites above 440 K. This temperature is still slightly below the superionic transition temperature. The deuteron spectrum thus exhibits a dynamic motional transition from the slow to fast motion regime, in complete analogy to the ^{87}Rb spectrum. The transition can be again associated with the SO_4 reorientations which dynamically average the local crystal symmetry determining the deuteron EFG tensor. The theoretical spectrum in Fig. 5 has been reproduced by the two-site exchange[17] model where the resonance frequency of deuterons stochastically changes between two values with the exchange frequency Ω_0. The temperature dependence of Ω_0 is displayed in Fig. 4 together with the values determined from the ^{87}Rb spectra. Both values fall on a straight line with the same activation energy demonstrating that the same motion is observed by the ionically bound Rb and the covalently bound deuteron nuclei. This in turn proves that the SO_4 reorientations induce the deuteron ionic transport. The inverse frequency $\Omega_0^{-1} = \tau_{exch}$ represents the average SO_4 reorientational time which also represents the average deuteron interbond transfer time determining its ionic mobility. Around 300 K the deuteron transfer is slow, $\tau_{exch} \approx 50$ ms, whereas at the superionic transition temperature 450 K it speeds up to 1.6×10^{-6} sec and continues to shorten on further heating.

It is interesting that inside the superionic phase a pair of deuteron satellite lines with a nonzero quadrupolar splitting still exists instead of a single line at the Larmor frequency (in the center of the spectrum) expected if the quadrupolar splitting would be averaged to zero. This demonstrates that the interbond motion is not isotropic in space since the isotropic motion would time-average the traceless electric quadrupole interaction to zero. The SO_4 and the associated deuteron motion is thus anisotropic in space which is consistent with the assumption that the SO_4 reorientations are performed about an axis which has a well defined direction in space. The superionic transport of deuterons thus involves motion over well defined lattice sites so that only some of the EFG tensor elements are averaged to zero. On the other hand, in a pure two-site exchange process with no accompanying change of the crystal symmetry, the absorption line in the fast motion limit should form at a time-averaged position of the two lines of the static spectrum, i.e. it should lie somewhere between these two lines. In Fig. 5 it is seen that the fast motion limit line is formed outside of this range, closer to the center of the spectrum than any of the two lines of the static spectrum. This effect reflects the macroscopic change of the crystal symmetry on going into the superionic phase.

C. Two-dimensional deuteron exchange NMR

The dynamic line-shape transition discussed in the preceding section demonstrates that the motion responsible for the superionic transport of deuterons exists already far below the actual superionic transition at 448 K. The ^{87}Rb and ^2H one-dimensional spectra become affected by this motion above about 350 K, when the motional frequencies become comparable to the line splitting, which is in the kHz range. In the following we demonstrate that the 2D exchange NMR spectra of deuterons give a direct evidence for the existence of slow SO_4 reorientations and the associated deuteron interbond transport already at room temperature, which is as much as ~170 K below the superionic phase transition. The thermally activated reorientations occur at this temperature on the sub-Hz frequency scale. 2D exchange NMR[18] detects the existence of slow spatial motion of the resonant nuclei between sites with different resonance frequency. When the exchange takes place during the mixing interval (t_{mix}) of the 2D experiment, the 2D spectrum exhibits cross peaks in the (ω_1, ω_2) plane which appear at the cross positions (ω_i, ω_j) to the diagonal peaks (ω_i, ω_i). The diagonal peaks correspond to the nuclear sites with different resonance frequencies. A given cross peak demonstrates that the deuteron

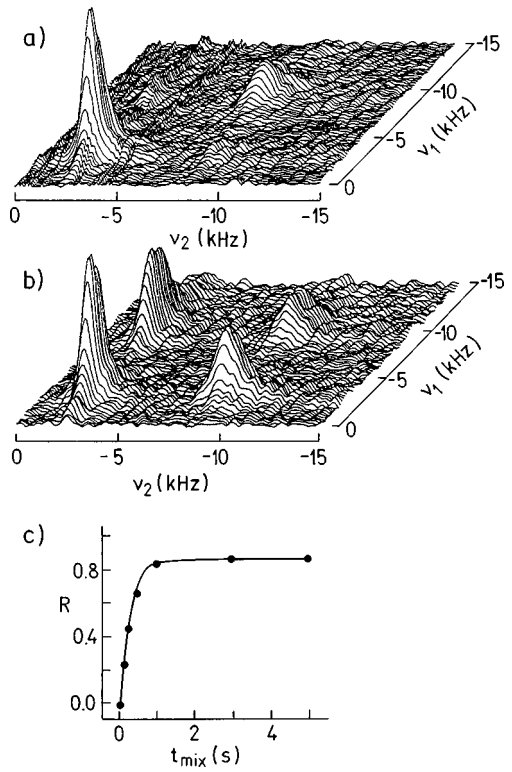

FIG. 6. Deuteron 2D exchange NMR spectrum at 290 K in $Rb_3D(SO_4)_2$ [(a) $t_{mix}=100$ ms, (b) $t_{mix}=5$ sec, (c) cross-to-diagonal peak intensity ratio R as a function of the mixing time]. The $1 \rightarrow 0$ satellite transitions are shown only.

transfer took place from one H bond to another with a different deuteron EFG tensor. The exchange time constant can be extracted by measuring the 2D exchange spectrum for a set of mixing times t_{mix} which determine the interval inside which the deuteron motion is monitored coherently. The dependence of the cross-to-diagonal peak intensities $R=\tanh(t_{mix}/\tau_{exch})$ on the mixing time yields the average interbond exchange time τ_{exch}.

The deuteron 2D exchange spectrum at 290 K is shown in Figs. 6(a) and 6(b). The cross-to-diagonal peak intensity ratio [Fig. 6(c)] yielded $\tau_{exch}=462$ ms so that the exchange frequency amounts to $\tau_{exch}^{-1}=2\pi\times 0.34$ Hz. This value again falls on a straight line with the Ω_0 values determined from the ^{87}Rb and ^{2}H 1D spectra (Fig. 4) and demonstrates that the same physical motion is observed in all cases.

The 2D exchange experiment thus shows that the SO_4 reorientation-induced deuteron ionic transport is present already at room temperature. In the following section we will show that the high elasticity of the $Rb_3D(SO_4)_2$ structure also contributes the dominant NMR spin-lattice relaxation mechanism in a broad temperature interval from the superionic phase down to as low as 20 K.

V. NMR SPIN-LATTICE RELAXATION

Another insight into the dynamics of the $Rb_3H(D)(SO_4)_2$ systems is provided by the NMR spin-lattice relaxation (T_1) experiment. Spin-lattice relaxation probes the dynamics on the frequency scale of the nuclear precession ($\sim 10^8$ Hz). The SO_4 rotational motions and the deuteron ionic transport observed in the ^{87}Rb and ^{2}H line shape and 2D exchange studies on the kHz and sub-kHz scales are thus too slow to affect the spin-lattice relaxation rate. T_1 of quadrupolar nuclei such as ^{87}Rb and ^{2}H is determined by the fluctuating part of the EFG tensor and the observed temperature and frequency dependence should allow for a discrimination between different possible relaxation mechanisms.

Spin-lattice relaxation rates were measured as a function of temperature in both $Rb_3H(SO_4)_2$ and $Rb_3D(SO_4)_2$ crystals on ^{87}Rb and ^{2}H nuclei. For ^{87}Rb nuclei ($I=\frac{3}{2}$) the two probabilities W_1 and W_2 of the spin transitions $\Delta m=\pm 1$ and $\Delta m=\pm 2$ have been determined from the magnetization-recovery curve $M(\tau)=M_0[1-(\exp\{-2W_1\tau\}+\exp\{-2W_2\tau\})]$ following the inversion of the central line. Only W_1 is discussed in the following due to a complete analogy with W_2. For deuterons the magnetization-recovery curve is monoexponential with the time constant $1/T_1=W_1+2W_2$.

The relaxation rates have been measured between the superionic phase and 4 K. The ^{87}Rb relaxation rates W_1 of $Rb_3H(SO_4)_2$ and $Rb_3D(SO_4)_2$ are displayed in Fig. 7(a) in the whole temperature range, whereas in Fig. 7(b) the rates are shown on an expanded temperature scale down to 17 K. The deuteron T_1 is shown in Fig. 7(c). The ^{87}Rb W_1^{-1} of $Rb_3H(SO_4)_2$ shows a monotonic increase on cooling. At high temperatures the rate—plotted on the $\ln W_1$ vs $1/T$ scale—shows a fast increase, whereas at lower temperatures the increase becomes slower and the rate shows a tendency to saturate at a T-independent value. The same overall behavior is observed also for the ^{87}Rb relaxation rate in the deuterated compound. At high temperatures W_1^{-1} shows identical fast increase with decreasing temperature and, moreover, its value is nearly the same as the one of the protonated compound. In the vicinity of the antiferroelectric transition at 82 K the relaxation rate shows a typical soft mode minimum. Below this transition W_1^{-1} increases and once again matches the values of the protonated compound at 30 K and then follows its temperature dependence down to about 17 K. This is shown in Fig. 7(b). Apart from the minimum at T_{c2} which occurs only for the deuterated compound, the general temperature dependence of the relaxation rates is the same in the protonated and the deuterated compounds. This demonstrates that the same dynamic process is rate determining in both cases. The minimum in the deuterated compound reflects the slowing down of the deuteron intra-H-bond motion which affects the relaxation rate only in the vicinity of T_{c2}. It seems that the soft mode relaxation is largely independent of the dynamic process producing the general temperature increase of the rates on cooling.

An identical situation is observed in the ^{2}H relaxation rate [Fig. 7(c)] in $Rb_3D(SO_4)_2$. The T_1 shows a similar general increase on cooling which is fast at high and slow at low temperatures. There is in fact a one-to-one correspondence to the ^{87}Rb relaxation rates. In the vicinity of T_{c2} the deuteron rate also shows a rather insignificant soft-mode minimum. The deuteron intrabond motion and the corresponding soft-mode relaxation again affect T_1 only in the vicinity of T_{c2} and is superimposed on the main relaxation mechanism, producing the general T_1 increase on cooling.

It is evident that the general temperature dependence of

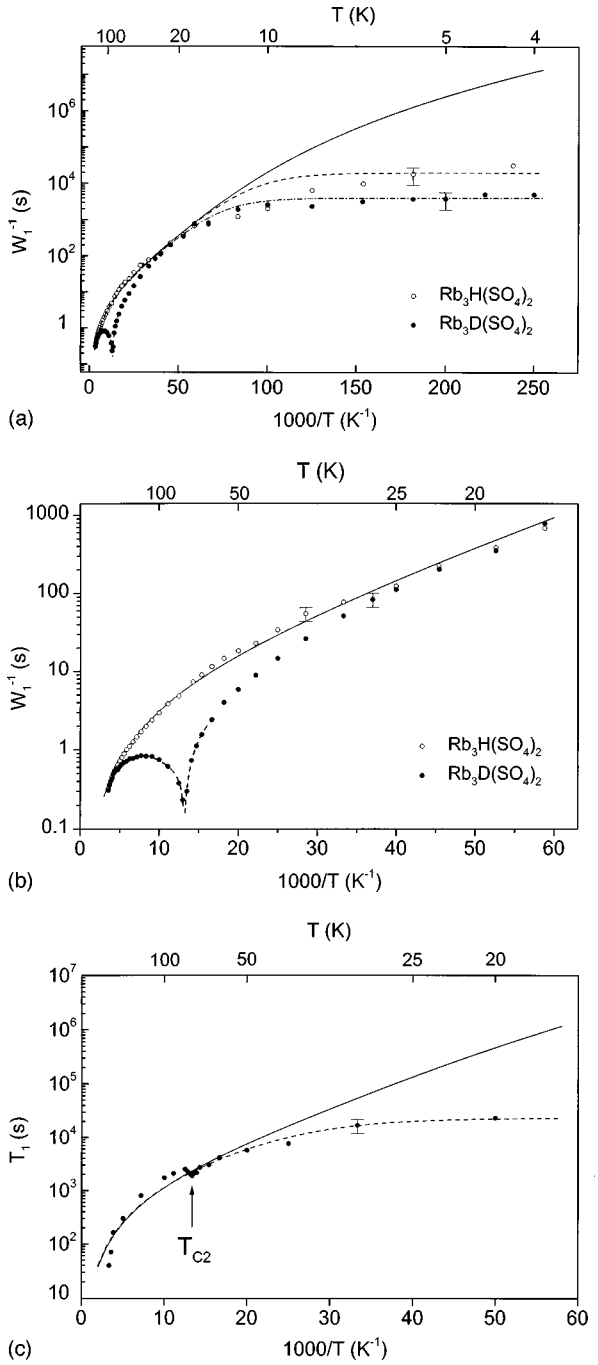

FIG. 7. (a)Temperature dependence of the ^{87}Rb relaxation rate W_1 in $Rb_3H(SO_4)_2$ and $Rb_3D(SO_4)_2$ between the superionic phase and 4 K [$\nu_0(^{87}\mathrm{Rb}) = 124.34$ MHz, $c_m \perp H_0$, $\angle a_m, H_0 = 15°$]. The solid line represents the fit with the model of lattice-vibrations-induced (Raman) relaxation [Eq. (1)]. The dashed and dash-dot lines represent fits with the same model with the addition of a temperature-independent relaxation mechanism at low temperatures [Eq. (2)]. (b) Same as in (a) but on an expanded temperature scale down to 17 K. In this temperature interval the Raman relaxation contribution solely (solid line) reproduces well the experimental points. The dotted line represents the fit of the W_1^{-1} minimum in the deuterated compound with the soft-mode term. (c) Temperature dependence of the deuteron relaxation time T_1 in $Rb_3D(SO_4)_2$ [$\nu_0(^2\mathrm{H}) = 58.3$ MHz, $c_m \perp H_0$, $a_m \| H_0$]. The solid line represents the fit with the Raman term only whereas dashed line represents the fit with both the Raman and the *T*-independent contributions.

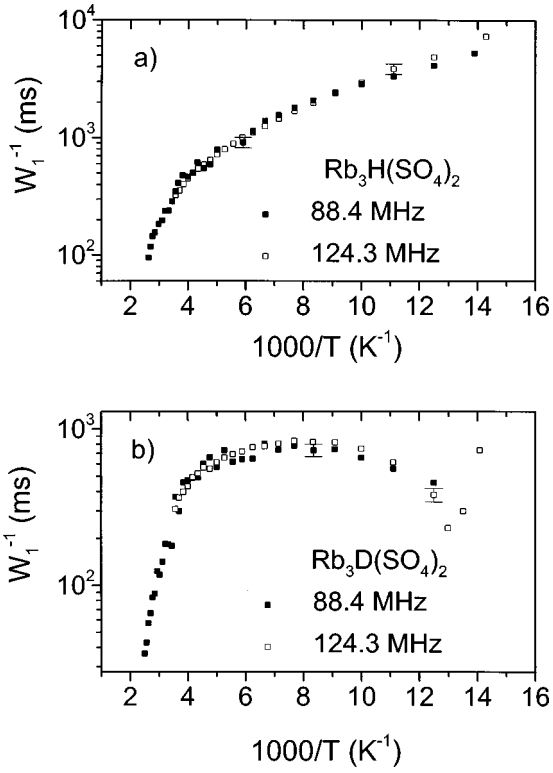

FIG. 8. ^{87}Rb relaxation rates in the interval between the superionic phase and 60 K in (a) $Rb_3H(SO_4)_2$ and (b) $Rb_3D(SO_4)_2$ measured at two Larmor frequencies 124.34 and 88.4 MHz.

the relaxation rates is the same in both the protonated and deuterated compounds. This is true both for the ionically bound ^{87}Rb and the covalently bound ^{2}H nuclei. It is also remarkable that the temperature dependencies of all the relaxation rates are so similar in a very large *T* interval ranging from the superionic phase down to the temperatures as low as 17 K, which is far below the antiferroelectric transition in the deuterated compound. Another striking feature is the independence of the relaxation rates on the nuclear Larmor frequency. In the standard Bloembergen-Purcell-Pound theory the relaxation rates induced by the stochastic random thermally induced motions, which slow down on cooling, are frequency independent only in the fast motion limit. There the molecular motions are fast on the Larmor frequency scale. When the temperature decreases, the inverse relaxation rate (T_1) also decreases and exhibits a minimum when the motional frequencies cross the nuclear Larmor frequency. Below the minimum the system is in the slow motion limit where the T_1 *increases* on cooling, but becomes *frequency dependent*. In our investigated systems we found a striking feature that T_1 *increases* with decreasing temperature, but is *frequency independent*. This is shown in Fig. 8 where the ^{87}Rb relaxation rates of $Rb_3H(SO_4)_2$ [Fig. 8(a)] and $Rb_3D(SO_4)_2$ [Fig. 8(b)] measured at two Larmor frequencies 124.34 and 88.4 MHz are displayed. A frequency-independent ^{87}Rb T_1 which increases with decreasing temperature was found also in the related compound $Rb_3H(SeO_4)_2$ (Ref. 15). This anomalous T_1 behavior can be explained by the relaxation mechanism of lattice vibrations coupled to the nuclear electric quadrupole moments with the dominating Raman processes[19] (absorption of one phonon ω

and emission of another ω'). Here the frequencies ω and ω' of the two phonons involved satisfy the energy conservation relation $\omega-\omega'=\omega_0$ (where ω_0 is the nuclear Larmor frequency) so that all phonons inside the phonon spectrum contribute to the relaxation processes. This makes the Raman-induced spin-lattice relaxation rate independent of the Larmor frequency. In the Debye approximation for the phonon density of states we get[19]

$$\left(\frac{1}{T_1}\right)_{\text{Raman}}=K\int_0^{\theta}\frac{\exp\{T'/T\}}{(\exp\{T'/T\}-1)^2}\left(\frac{T'}{\theta}\right)^6 dT', \qquad (1)$$

where θ is the Debye temperature. For $T\geqslant\theta$ we get $T_1^{-1}\propto T^2$, whereas at very low temperatures ($T/\theta\ll 0.02$) this dependence is $T_1^{-1}\propto T^7$. The phonon-induced relaxation is commonly found in electron spin resonance spin-lattice relaxation but very rare in nuclear spin relaxation.

The ^{87}Rb W_1 of $Rb_3H(SO_4)_2$ can be well reproduced with Eq. (1) in a large temperature range between the superionic phase and 17 K [solid lines in Figs. 7(a) and 7(b)]. The only fit parameter is the Debye temperature which is obtained as $\theta=150\pm 20$ K. In Fig. 7(a) it is observed that Eq. (1) (solid line) reproduces well the experimental points down to 17 K whereas below that temperature the experimental data start to deviate considerably from the theoretical fit. Below 10 K the experimental points form a temperature-independent plateau whereas in the model of Raman-induced relaxation W_1^{-1} continues to grow. It is obvious that another relaxation mechanism sets in at these temperatures and is responsible for the leveling-off of the relaxation rates. One possibility is spin diffusion to paramagnetic impurities and the other the presence of deuteron tunneling within the H bonds which also produces a plateau in T_1 at low temperatures.[20] The leveling off can be reproduced qualitatively by assuming the existence of a temperature-independent relaxation contribution $(1/T_1)_T$ which adds to the Raman rate

$$\frac{1}{T_1}=\left(\frac{1}{T_1}\right)_{\text{Raman}}+\left(\frac{1}{T_1}\right)_T. \qquad (2)$$

Equation (2) now reproduces the experimental rates down to the lowest measured temperatures of 4 K. For $Rb_3H(SO_4)_2$ the fit procedure [dashed line in Fig. 7(a)] yielded $[(1/T_1)_T]^{-1}=1.06\times 10^4$ sec. It should be emphasized that the temperature-independent contribution is needed only to reproduce the plateaus below 10 K, whereas it has no effect on the relaxation rates above 17 K. Above that temperature the lattice vibrations dominate the spin-lattice relaxation.

Equation (2) also reproduces the general temperature dependence (without the minimum) of T_1 in the deuterated compound [dash-dot line in Fig. 7(a)]. The fit yields the same Debye temperature $\theta=150$ K and $[(1/T_1)_T]^{-1}=4\times 10^3$ sec. The minimum at T_{c2} can be accounted qualitatively by the deuteron intrabond motion resulting in a soft-mode contribution to the relaxation $1/T_1=A/|T_{c2}-T|^{\beta}$ which is added to Eq. (2). In our fit procedure this term has been taken into account only in the vicinity of the phase transition and neglected outside of this region [dashed line in Fig. 7(b)]. The experimental precision did not allow us to determine accurately the power law exponent which was taken in the fit as $\beta\approx 0.5\pm 0.2$.

Equation (2) reproduces equally well also the deuteron T_1 in $Rb_3D(SO_4)_2$ [dashed line in Fig. 7(c)] with $\theta=155$ K and $[(1/T_1)_T]^{-1}=2.33\times 10^4$ sec. The solid line in Fig. 7(c) shows only the Raman contribution to the relaxation. The sole Raman contribution again reproduces correctly the data in the high-T region down to about 50 K which is considerably below the antiferroelectric phase transition.

In order to find out the nature of the relaxation mechanism below 17 K we performed a measurement of the ^{87}Rb and ^{85}Rb relaxation rates at 6.5 K in both $Rb_3H(SO_4)_2$ and $Rb_3D(SO_4)_2$ compounds. There are three important differences between the ^{87}Rb and ^{85}Rb isotopes. ^{87}Rb (spin $I=\frac{3}{2}$) has a 3.4 times larger nuclear magnetic dipole moment than ^{85}Rb ($I=\frac{5}{2}$). The nuclear electric quadrupole moment of ^{87}Rb is, however, smaller than that of ^{85}Rb: $Q(^{87}\text{Rb})/Q(^{85}\text{Rb})=0.48$. The two isotopes also appear in different natural abundance ($n^{87}=27.8\%$ and $n^{85}=72.2\%$) so that the average distance between the ^{87}Rb nuclei ($r^{87}=\sqrt[3]{1/n^{87}}$) is larger than that between the ^{85}Rb nuclei, $r^{87}/r^{85}=1.37$. These differences allow us to discriminate between the electric quadrupolar (vibrations-induced or tunneling) relaxation and spin diffusion to paramagnetic impurities of magnetic dipolar origin.

The ratio of the spin diffusion rates can be estimated by the theory of Abragam.[21] One gets $T_1^{\text{SD}}(^{85}\text{Rb})/T_1^{\text{SD}}(^{87}\text{Rb})\approx 10$ so that the ^{87}Rb isotope should show a $\approx$10 times faster spin-diffusion-induced relaxation rate than the ^{85}Rb isotope. On the other hand, the electric quadrupole-induced relaxation of ^{87}Rb is about 20 times slower than that of ^{85}Rb, $T_1^Q(^{85}\text{Rb})/T_1^Q(^{87}\text{Rb})\approx 0.02$.

The magnetization-recovery curves $M(\tau)$ of ^{87}Rb and ^{85}Rb at 6.5 K (not shown) were measured under the same experimental conditions. Both relaxation curves were found practically identical in the protonated compound, whereas there was only an insignificant difference in the deuterated compound. In view of the above differences between the ^{87}Rb and ^{85}Rb isotopes this result is only possible if both types of relaxation—the electric quadrupolar and the spin diffusion—are present simultaneously with a similar relaxation strength. This is an unfavorable situation as the presence of spin diffusion obscures the relaxation induced by molecular dynamics and makes the analysis at low-T ambiguous. Here we mention that the same ^{87}Rb/^{85}Rb comparison of $M(\tau)$ curves in proton glasses DRADP and RADP showed[20] that the ^{85}Rb relaxation was much faster under the same experimental conditions so that the electric quadrupole nature (due to phonon-assisted tunneling) of the spin-lattice relaxation at low temperatures was unambiguously identified.

VI. CONCLUSIONS

NMR line shape and spin-lattice relaxation measurements have shown that the dynamics of $Rb_3H(SO_4)_2$ and $Rb_3D(SO_4)_2$ is predominantly determined by the thermally induced SO_4 vibrations, torsional oscillations, and reorientations resulting from the high elasticity of the crystal structure. The SO_4 reorientations are accompanied by the proton interbond transfer which results in ionic conductivity. In addition the deuteron intrabond motion resulting in a soft-mode

dynamics has been observed in the vicinity of the antiferroelectric transition in the deuterated compound. T_1 measurements have shown that lattice vibrations dominate the spin-lattice relaxation in a large temperature interval from the superionic phase down to as low as about 20 K. Likewise 2D exchange NMR has detected the deuteron interbond motion as a precursor of the superionic conductivity already at room *T*. This is as much as 170 K below the actual superionic phase transition. The high elasticity of the lattice is responsible for the occurrence of the superionic conducting phase at high *T* and seems to also play an important role in the suppression of the phase transition in the protonated compound at low *T*. The phonons induce proton intrabond motion over the excited states which appears intense enough to suppress the transition. This proton transfer mechanism is much less efficient in the deuterated compound where the H-bond length is larger and the barrier is higher so that the transition is preserved. The anomalously high elasticity of the crystal structure together with the accidentally short protonated H-bond length thus seem to be responsible for the lack of proton ordering in $Rb_3H(SO_4)_2$.

ACKNOWLEDGMENT

We would like to thank Dr. Andreas Titze from Johannes Gutenberg University, Mainz for providing us the manuscript on the ^{87}Rb NMR study of the antiferroelectric transition in $Rb_3D(SO_4)_2$ prior to publication.

[1] K. Gesi, J. Phys. Soc. Jpn. **48**, 886 (1980).
[2] Y. Moritomo, Y. Tokura, N. Nagaosa, T. Suzuki, and K. Kumagai, Phys. Rev. Lett. **71**, 2833 (1993).
[3] P. Kaung, M. Kasahara, and T. Yagi, J. Phys. Soc. Jpn. **65**, 1114 (1996).
[4] K. Gesi, J. Phys. Soc. Jpn. **61**, 162 (1992).
[5] C. Totsuji and T. Matsubara, Solid State Commun. **89**, 677 (1994).
[6] Y. Noda and H. Kasatani, J. Phys. Soc. Jpn. **60**, 13 (1991).
[7] Y. Noda, H. Kasatani, Y. Watanabe, and H. Terauchi, J. Phys. Soc. Jpn. **61**, 905 (1992).
[8] Y. Noda, Y. Watanabe, H. Kasatani, H. Terauchi, and K. Gesi, J. Phys. Soc. Jpn. **60**, 1972 (1991).
[9] M. Ichikawa, T. Gustafsson, K. Motida, I. Olovsson, and K. Gesi, Ferroelectrics **108**, 307 (1990).
[10] M. Ichikawa, T. Gustafsson, and I. Olovsson, Solid State Commun. **87**, 349 (1993).
[11] S. Takeda, F. Kondoh, N. Nakamura, and K. Yamaguchi, Physica B **226**, 157 (1996).
[12] F. Fillaux, A. Lautie, J. Tomkinson, and G. J. Kearley, Chem. Phys. **154**, 135 (1991).
[13] I. P. Makarova, L. A. Shuvalov, and V. I. Simonov, Ferroelectrics **79**, 111 (1988).
[14] N. M. Plakida and W. Salejda, Phys. Status Solidi B **148**, 473 (1988).
[15] D. Abramič, J. Dolinšek, R. Blinc, and L. A. Shuvalov, Phys. Rev. B **42**, 442 (1990).
[16] Y. Noda, I. Tamura, H. Nakao, R. Matsuo, and Y. Kuroiwa, J. Phys. Soc. Jpn. **63**, 1803 (1994).
[17] A. Abragam, *The Principles of Nuclear Magnetism* (Oxford University Press, Oxford, 1961), p. 447.
[18] See, e.g., R. R. Ernst, G. Bodenhausen, and A. Wokaun, *Principles of Nuclear Magnetic Resonance in One and Two Dimensions* (Clarendon, Oxford, 1987), p. 490.
[19] A. Abragam, *The Principles of Nuclear Magnetism* (Ref. 17), p. 401.
[20] J. Dolinšek, D. Arčon, B. Zalar, R. Pirc, R. Blinc, and R. Kind, Phys. Rev. B **54**, R6811 (1996).
[21] A. Abragam, *The Principles of Nuclear Magnetism* (Ref. 17), p. 385.